Results in Engineering 25 (2025) 104337

Contents lists available at ScienceDirect

Results in Engineering

journal homepage: www.sciencedirect.com/journal/results-in-engineering

A novel CPW-fed flexible antenna with circular polarization for enhanced vehicular communication systems

Rajesh Kumar D [a], Vaithianathan Venkatesan [b], Raja Periyasamy [c], B. Rubini [d], Ragunath G [e], Om Prakash Kumar [f], Shweta Vincent [g,*]

[a] Department of Electronics and Communication Engineering, Vel Tech Rangarajan Dr. Sagunthala R&D Institute of Science and Technology, India
[b] Department of Electronics and Communication Engineering, Sri Sivasubramaniya Nadar College of Engineering, India
[c] Department of Electronics and Communication Engineering Sri Manakula Vinayagar Engineering College, India
[d] Department of Electronics and Communication Engineering Vels Institute of Science Technology and Advanced Studies, India
[e] School of Electronics Engineering, Vellore Institute of Technology, Vellor, India
[f] Department of Electronics and Communication Engineering, Manipal Institute of Technology, Manipal Academy of Higher Education, Manipal 576104, India
[g] Department of Mechatronics, Manipal Institute of Technology, Manipal Academy of Higher Education, Manipal 576104, India

ARTICLE INFO

Keywords:
Flexible
Conformal
Vehicular
Axial ratio
Circular polarization
SDG 9
SDG 11

ABSTRACT

The rapid proliferation of advanced technology and the Internet of Things (IoT) has driven significant innovation in the design and development of flexible sensor antennas. This paper introduces a novel, highly flexible coplanar waveguide (CPW)-fed antenna tailored for vehicular applications. With a compact form factor of 27.5 × 53 × 0.1 mm^3, the antenna demonstrates a broad impedance bandwidth of 5.5 to 6.5 GHz and a peak gain of 4.45 dBi, making it ideal for high-performance communication systems. A thorough bending analysis under various radii reveals robust flexibility and consistent performance, showcasing the antenna's adaptability to diverse operating conditions. The fabricated prototype exhibits excellent agreement between measured and simulated results, including a 100 % axial ratio bandwidth (ARBW), ensuring optimal circular polarization. These findings confirm the antenna's efficacy and reliability, making it a strong candidate for future vehicular communication systems.

1. Introduction

In recent years, flexible antennas have emerged as a significant research focus due to their potential in the Internet of Things (IoT), biomedical applications, conformal devices, and wearable electronics. Unlike conventional rigid antennas, flexible antennas are engineered to function effectively even when they are bent, stretched, or twisted, rendering them an ideal choice for integration into non-planar surfaces [1,2]. The selection of flexible substrates, such as polyimide, PDMS (polydimethylsiloxane), and PET (polyethylene terephthalate), is essential for their functionality. These polymers are both lightweight and durable. These materials enable antennas to maintain their electrical properties while simultaneously offering mechanical flexibility [3,4]. The radiating elements are created using conductive inks, which are typically made of silver, copper, or carbon-based materials. This allows for the direct printing of antennas onto malleable substrates [5]. The development of more robust and extremely stretchable antennas has been facilitated by the advancements in nanomaterials, such as graphene, which have opened up new possibilities due to their exceptional mechanical properties and conductivity [6]. Coplanar waveguide (CPW) structures have been implemented in recent designs, which provide flexibility by reducing the impact of substrate deformation on the antenna's performance [7]. Other strategies involve employing serpentine or meandered structures, which enable the antenna to expand without substantially altering its resonant characteristics [8]. Circularly polarised (CP) antennas, in particular, are attracting attention for their capacity to maintain consistent performance in the face of physical deformations [9]. Under various deformation conditions, the performance of flexible antennas is assessed using metrics such as impedance matching, gain, efficiency, and radiation patterns [2,7]. Nevertheless, obstacles persist, including the need to guarantee consistent performance in a variety of bending conditions and to achieve sufficient durability for long-term use [4,9]. The versatility and increasing relevance of flexible antennas in the 5 G and beyond communication era are evidenced by their exploration in a variety of applications, including body-worn antennas in healthcare devices and

* Correspondence author.
E-mail address: shweta.vincent@manipal.edu (S. Vincent).

https://doi.org/10.1016/j.rineng.2025.104337
Received 16 November 2024; Received in revised form 31 January 2025; Accepted 10 February 2025
Available online 13 February 2025

conformal antennas on drones and vehicles [1,3]. This discipline is swiftly evolving and dynamic, as recent research continues to emphasise the enhancement of flexibility without sacrificing efficacy [6,8]. The potential of flexible antennas to improve automotive and transportation technologies' communication systems is drawing a lot of attention to them for use in vehicles. Especially in vehicles where aerodynamic design, space limits, and durability under mechanical stress are crucial aspects, traditional stiff antennas often confront integration issues. Flexible antennas provide a viable remedy for these problems because of their capacity to adapt to the curved surfaces of automobiles [10,11]. Flexible antennas' capacity to continue operating at a constant level in the face of mechanical deformation brought on by road conditions, vibrations, and changes in vehicle shape as a result of load and stress is one of their fundamental benefits for automotive applications. For applications like automotive radar, vehicle-to-everything (V2X) connectivity, and in-vehicle wireless networks, this makes them perfect [12,13]. Furthermore, the integration of these antennas into other vehicle surfaces, such mirrors, windscreens, and bumpers, may be done without sacrificing the aerodynamics or aesthetics of the vehicle [14]. Their versatility in operating over a broad frequency range is another important asset, as it makes them appropriate for future vehicle networks and low- and high-frequency communication systems, such as 5 G [15,16]. En-Naghma et al. [17] proposed a highly efficient dual-band rectenna system optimized using genetic algorithms for RF energy harvesting applications. Their work highlighted the importance of advanced optimization techniques to achieve high efficiency in energy harvesting. Further, the same authors extended their research to develop a novel triple-band microstrip antenna based on a hexagonal patch design with ground truncation [18]. This design demonstrated improved performance for RF energy harvesting systems, showcasing the benefits of innovative patch shapes and ground plane modifications. Additionally, En-Naghma et.al explored designing and optimizing dual-band microstrip antennas using genetic algorithms [19]. Their research contributed to understanding how optimization algorithms can effectively enhance antenna characteristics for energy-harvesting applications. The push for wearable and flexible antenna solutions for emerging technologies like 5 G has also been a recent research focus. John et al. [20] presented a wideband, highly flexible coplanar waveguide (CPW)-fed antenna based on characteristic mode analysis for wearable sensor applications. This study emphasized the role of flexibility and wideband capabilities in meeting the requirements of 5 G wireless systems. In the realm of biomedical applications, Didi et al. [21] designed a soft circular patch antenna operating at 2.45 GHz for 5G. Their work demonstrated the potential of soft materials in creating bio-compatible antennas, suitable for medical devices and wearable sensors.

The literature survey highlights several advancements and challenges in the development of flexible antennas, especially their potential use in IoT, wearable electronics, biomedical applications, and automotive sectors. However, it emphasizes several persistent obstacles, particularly the need to ensure consistent performance under mechanical deformation (e.g., bending, stretching) and to improve long-term durability under environmental factors like UV rays, humidity, and temperature changes. It also points out challenges in guaranteeing stable performance in automotive applications, such as addressing aerodynamic design limitations and mechanical stressors like vibrations. Overall, the gap lies in the need for antennas that are highly durable, flexible under mechanical stresses, and maintain efficient performance across different conditions.

This article addresses this research gap by introducing a novel CPW-fed antenna specifically designed for vehicular applications, which appears to overcome the challenges outlined in the first paragraph. The antenna is compact and demonstrates broad impedance bandwidth, high gain, and consistent performance under mechanical bending, as shown through bending analysis. Furthermore, the design features 100 % axial ratio bandwidth, ensuring stable circular polarization and thus maintaining performance despite physical deformation. This shows a step forward in developing antennas that can withstand various operating conditions and mechanical stresses, effectively overcoming some of the challenges in durability and flexibility.

The research article is organized into several distinct sections to provide a comprehensive view of the antenna design and its performance. The Proposed Antenna Design and Analysis section introduces the design's conceptual foundation, structural components, and theoretical basis. Following this, the Results and Discussions section presents detailed analyses of the simulated results, discussing key performance metrics and design insights. The Measured Results and Discussion section compares the simulated findings with measured data, evaluating the antenna's performance in real-world conditions and its alignment with theoretical predictions. Lastly, the Conformal Analysis section explores the antenna's behavior when applied to conformal surfaces, assessing its adaptability and functional integrity in various practical scenarios.

The major contributions of the article are listed below:

1. High Flexibility and Robust Performance: The antenna shows resilience and stable performance under different curvature radii through comprehensive bending analysis, underscoring its suitability for dynamic vehicular environments.
2. Compact Design with High Efficiency: With a small footprint of 27.5 $\times$ 53 $\times$ 0.1 mm^3, the antenna fits seamlessly into space-constrained areas, an essential factor for modern vehicular systems that require unobtrusive integration without compromising performance.
3. Broad Impedance Bandwidth and Circular Polarization: Operating over the 5.5 to 6.5 GHz range with a peak gain of 4.45 dBi and achieving 100 % axial ratio bandwidth, the antenna supports reliable, high-speed communication with circular polarization. This is critical for vehicular communications where consistent signal quality is vital, especially in multipath environments.
4. Proven Reliability through Fabrication and Testing: The strong alignment between simulated and measured results highlights the design's practical viability, enhancing its attractiveness for real-world deployment.

1.1. Proposed antenna design and analysis

Fig. 1 presents a detailed structure and dimensions of a proposed flexible antenna, highlighting its key components: the blue CPW (Coplanar Waveguide) antenna and the yellow substrate. The antenna design features a circular radiating patch with a floral pattern, connected to a CPW feedline that extends from the patch to the antenna's edge. The annotated dimensions, such as W, L, R1, and L1, correspond to the overall size of the antenna, the patch radius, and the feedline's length and width, respectively.

The closer view of the circular radiating patch and the floral structure of the flexible antenna is also shown in Fig. 1. The left image zooms in on the circular patch, which features a detailed floral pattern, to enhance circular polarization characteristics. The patch is placed centrally on the substrate, and its diameter is denoted by the dimension L3, giving insight into the overall size of the radiating element. The right image focuses on the floral section, where L4 indicates the length of the floral structure. The narrow part of the CPW feedline is marked by W2, which defines the gap between the signal line and the surrounding ground planes. This configuration helps optimize the antenna's impedance and ensures efficient signal transmission. These close-up images illustrate the critical design elements that contribute to the antenna's flexible and functional nature. The CPW feeding method ensures simple fabrication and efficient performance, while the decorative circular patch could enhance radiation properties and contribute to a circularly polarized pattern. This structure emphasizes both aesthetic design and functionality, suitable for modern applications in flexible electronics and wireless systems. All the design parameters are listed in Table 1.

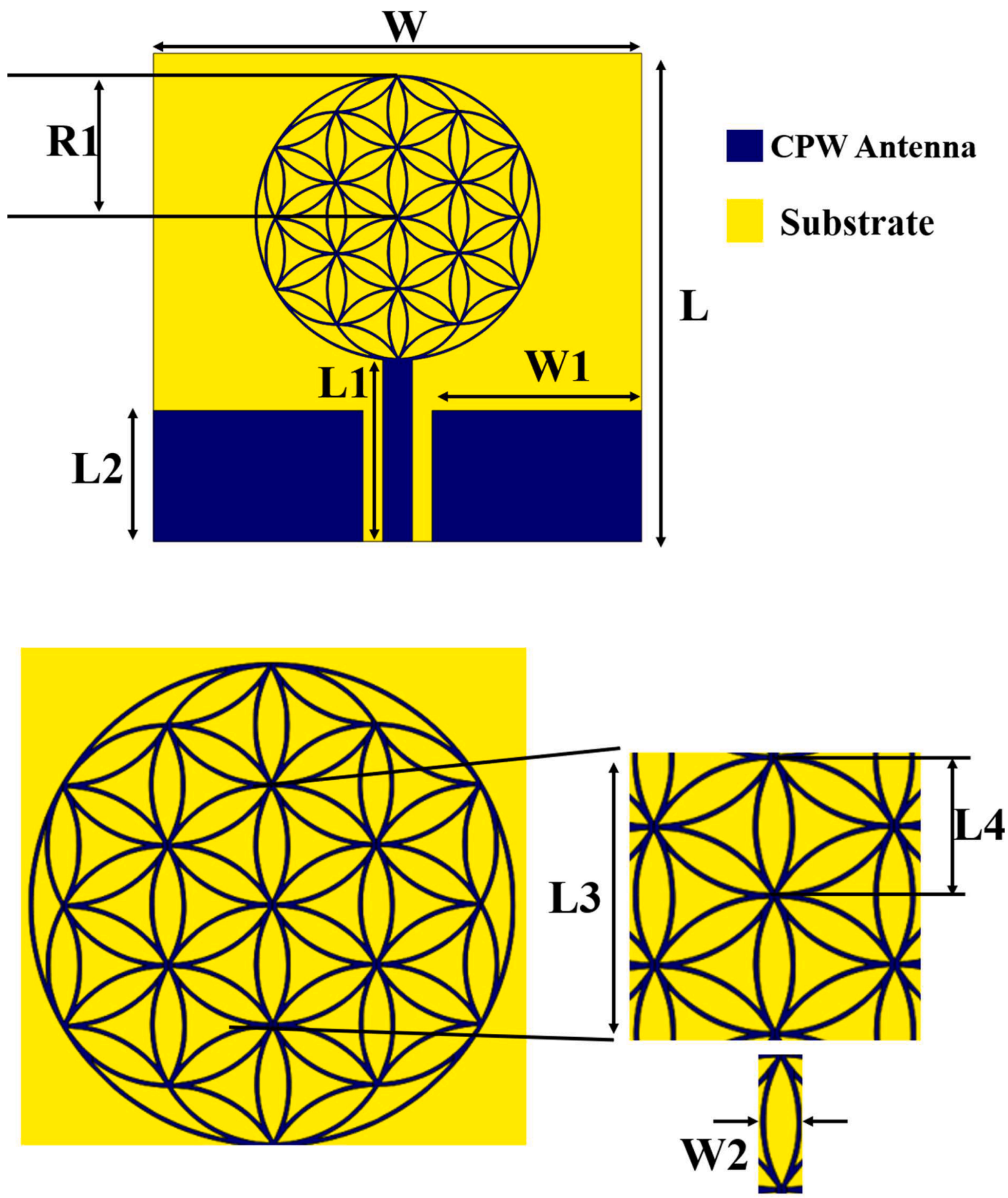

Fig. 1. Detailed structure and dimension of proposed flexible antenna.

Table 1
Various parameters of the proposed antenna.

Parameters	L	L1	L2	L3	L4	W	W1
Values (mm)	53	20.4584	12.741	16	8	27.5	23.6143

The following Eqs. (1)-(2) characterize the design formulation of the proposed CPW antenna.

Length of the ground plane (L1):

The length of the ground plane L2 is typically based on the operating wavelength λ. A common guideline is that the ground plane should be at least one-fourth of the wavelength (λ/4\lambda/4λ/4) or longer, depending on the specific application and design requirements.

$$L2 = n.\frac{\lambda}{4} \tag{1}$$

where:

- λ is the wavelength of the operating frequency.
- n is a factor usually taken as 1 or more, depending on how much extension beyond λ/4 is required for the design stability.

Feed Line Length (L2) calculation:

CPW antennas are frequently chosen due to their advantageous characteristics, such as a low profile, ease of manufacturing, and capability to operate across a wide bandwidth. The size of these antennas is generally dictated by transmission line theory, which considers various factors, including resonant frequency, substrate properties, and geometric dimensions. By utilizing the effective electrical length of the antenna, defined by its circumference, one can approximate the resonant frequency of a circular CPW antenna.

$$\textit{Resonant frequency } (f_r) = \frac{c}{2\pi r_{eff}} \tag{2}$$

Where:
f_r = *resonant frequency*
c = *Speed of light*

r_{eff} = effective radius of the circular CPW antenna

The characteristic impedance of the CPW antenna is given by,

$$Z_0 = \frac{60}{\sqrt{\xi_{eff}}} \ln\left(\frac{4h}{w}\right)$$

ξ_{eff} = the effective dielectric constant of the substrate material,
h = height of the substrate
w = width of CPW trace

Fig. 2 illustrates a parametric study of an antenna's performance, focusing on the reflection coefficient (S11) across the operating frequency range. In Fig. 2(a), varying the ground plane length (L2) from 12.741 mm to 16.741 mm affects the resonance characteristics; notably, the proposed design (L2 = 13.741 mm) shows an optimal reflection coefficient, indicating better impedance matching and bandwidth compared to the other lengths. In Fig. 2(b), the feed length (L1) is altered, with the proposed length (L1 = 20.4584 mm) demonstrating the best performance in terms of low reflection coefficients around the resonant frequency. Overall, both parameters significantly influence the antenna's ability to efficiently radiate energy, with the ideal configurations yielding reflection coefficients below −10 dB, suggesting effective performance within the targeted frequency range.'

2. Results and discussions

Fig. 3(a) illustrates the evolution of an antenna design across three iterations, showcasing enhancements aimed at optimizing performance. Iteration 1 features a simple circular patch antenna, which, while easy to manufacture, did not meet the impedance matching and bandwidth requirements for required applications. In Iteration 2, a more complex geometry is introduced, resembling a modified circular patch with additional contours, potentially improving bandwidth and gain by increasing surface area. Finally, Iteration 3 (Proposed) presents an intricate geometric pattern akin circular floral pattern, which enhances impedance matching and radiation characteristics. This progression reflects a systematic design optimization strategy, where increasing geometric complexity is leveraged to achieve superior operational capabilities, ultimately resulting in better efficiency and broader bandwidth for the antenna.

Fig. 3(b) illustrates the reflection coefficient (S11) for three iterations of an antenna design over a frequency range of 5.6 to 6.6 GHz, reflecting each design's impedance-matching performance. Iteration 1 (black solid line) shows a relatively high reflection coefficient, particularly around the resonant frequency of approximately 6.1 GHz, indicating poor impedance matching with values above −10 dB. Iteration 2 (red dotted line) demonstrates some improvement but still fails to achieve optimal performance, as it remains above −10 dB in the targeted frequency range. In contrast, Iteration 3 (Proposed) (blue solid line) exhibits the best performance, with the reflection coefficient dropping below −10 dB across a broader bandwidth, suggesting effective impedance matching and enhanced efficiency in radiating or receiving energy. This progression highlights the successful iterative design process that optimizes the antenna's characteristics for superior operational performance within the specified frequency range.

Fig. 3(c) presents the progression of circular polarization performance across three iterations of an antenna design. In Iteration 1, the radiation patterns for both Left-Hand Circular Polarization (LHCP) and Right-Hand Circular Polarization (RHCP) exhibit broad, quasi-omnidirectional characteristics, with balanced coverage across most angles but limited polarization selectivity. Iteration 2 shows slight improvements, with smoother patterns and a marginal increase in gain, but the separation between LHCP and RHCP remains minimal, indicating the circular polarization is still weak. The proposed design (Iteration 3) demonstrates significant improvements, with a distinct separation between LHCP and RHCP at critical angles and a more directional radiation pattern. This iteration achieves better circular polarization, favouring one mode over the other, along with enhanced directivity, making it the most effective design for achieving strong circular polarization performance. Fig. 4 demonstrates the operating mechanism of circular polarization of the proposed antenna with different phase angles.

The surface current distribution of the proposed circularly polarized (CP) antenna, as shown in the figure, demonstrates a well-distributed and symmetrical current flow across the antenna at various angles (0°, 90°, 180°, and 270°). This rotation of currents is critical for generating circular polarization. Specifically, the symmetry and consistent pattern across different angles suggest that the currents maintain their rotation over a 360° cycle, a necessary condition for achieving circular polarization. Furthermore, the intensity variation (depicted in the color scale) shows that the antenna radiates energy consistently in multiple directions, which aligns with the typical characteristics of a circularly polarized antenna, confirming that both left-hand and right-hand circular polarizations can be supported by this design. The balanced current distribution and rotation over these key phases support the generation of circular polarization in the proposed antenna.

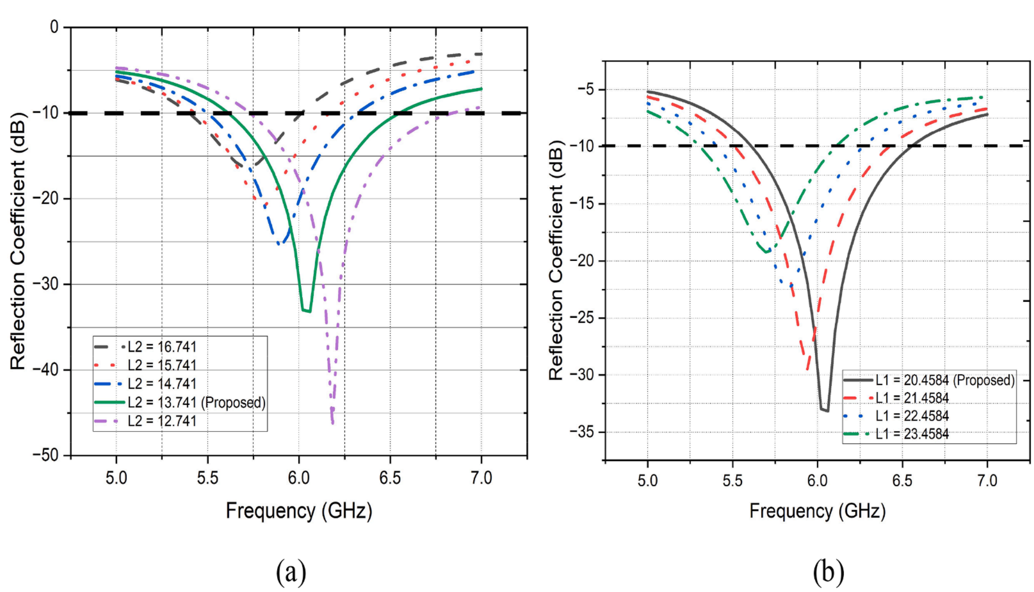

Fig. 2. Parametric study while altering (a) Ground plane length (L2), and (b) Feed length (L1).

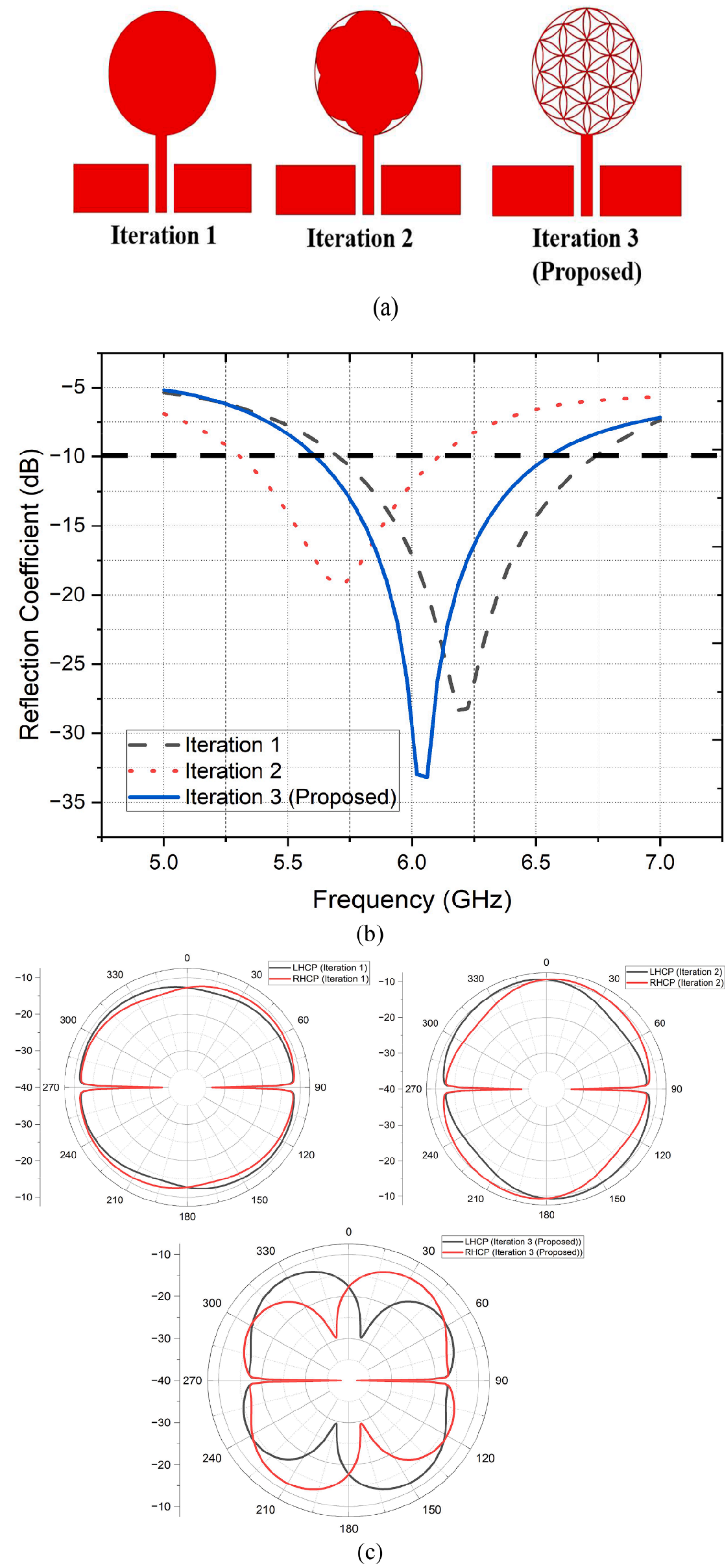

Fig. 3. (a) Design iterations of the proposed antenna, (b) Reflection coefficient of design iterations, and (c) Far-field patterns of design iterations.

2.1. Measured results and discussion

Fig. 5(a) illustrates a fabricated prototype of the proposed antenna printed on a 0.1 mm thick polyimide substrate. Fig. 5(b) shows the proposed antenna's reflection coefficient (S11), comparing simulated and measured results over the operating frequency range. The antenna operates effectively around 6.0 GHz, where both the simulated (black curve) and measured (red curve) results show a significant dip in the

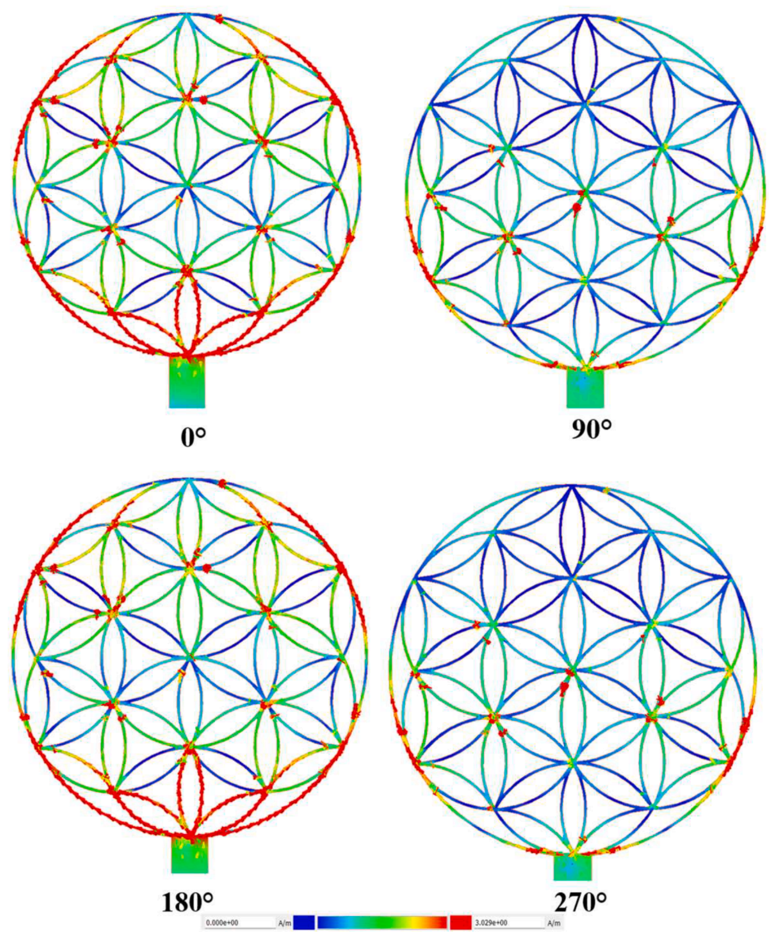

Fig. 4. Surface current distribution of the proposed antenna at different phase.

reflection coefficient, indicating good impedance matching. While minor imperfections are present in the fabricated prototype, particularly in the central floral structure, the overall performance remains consistent with the simulated results. The measured reflection coefficient aligns well with the simulations, demonstrating the reliability of the proposed antenna. These minor fabrication variations have a minimal impact on key performance parameters, indicating the robustness of the design. Future fabrication refinements will focus on improving precision to further enhance performance. The reflection coefficient dips below −10 dB between approximately 5.7 GHz and 6.5 GHz, providing a wide operational bandwidth of about 800 MHz. The simulated result achieves a minimum reflection coefficient of around −35 dB, while the measured result shows a slightly higher value, likely due to fabrication imperfections or measurement inaccuracies.

Fig. 6 presents the simulated and measured far-field radiation patterns for the antenna's right-hand circular polarization (RHCP) and left-hand circular polarization (LHCP) components. The RHCP (solid red for simulated, green for measured) shows a strong, well-defined pattern, confirming the antenna's effective circular polarization. The LHCP (dashed black for simulated, blue for measured) indicates minimal cross-polarization, highlighting good polarization purity and isolation. There is a close correlation between the simulated and measured patterns, though minor discrepancies can be observed, likely due to fabrication tolerances and measurement conditions. The antenna exhibits stable performance, confirming its suitability for environments requiring precise polarization control, such as in advanced wireless communication systems.

Fig. 7(a) and (b) compares the simulated and measured performance of the proposed antenna in terms of gain and axial ratio respectively. In Fig. 7(a), the simulated gain increases from around 4.2 dBi at 5.5 GHz to 5.3 dBi at 6.5 GHz, indicating strong performance across the band. However, the measured gain is lower, peaking at around 4.4 dBi near 6.0 GHz, likely due to fabrication and material losses affecting efficiency. In Fig. 7(b), both simulated and measured results remain below 3 dB between 5.7 GHz and 6.5 GHz, confirming the antenna's effective circular polarization in this band. Despite minor deviations, the close agreement between the simulated and measured axial ratios demonstrates the antenna's successful polarization characteristics and robust design.

2.2. Conformal analysis

Fig. 8 shows a flexibility analysis of a proposed antenna design, illustrating its behaviour under different bending angles: 30°, 45°, and 60°. The antenna is designed to maintain its integrity and performance even when bent. As the angle increases from 30° to 60°, the antenna's structural deformation adapts without significant changes in its overall mesh pattern. This suggests that the antenna's design is optimized to remain functional and resilient under varying mechanical stress, which is crucial for flexible and wearable applications where maintaining signal integrity during bending or twisting is essential.

Fig. 9(a) and (b) present the conformal analysis of the proposed antenna, focusing on its reflection coefficient and gain under various bending conditions (0°, 30°, 45°, and 60°). In Fig. 9(a), demonstrates that the antenna maintains effective impedance matching across all bending angles, with a minimum reflection coefficient close to −30 dB around 6 GHz. This behaviour indicates efficient performance and minimal signal loss within this frequency range, even when the antenna undergoes bending. The similarity of the curves across different angles

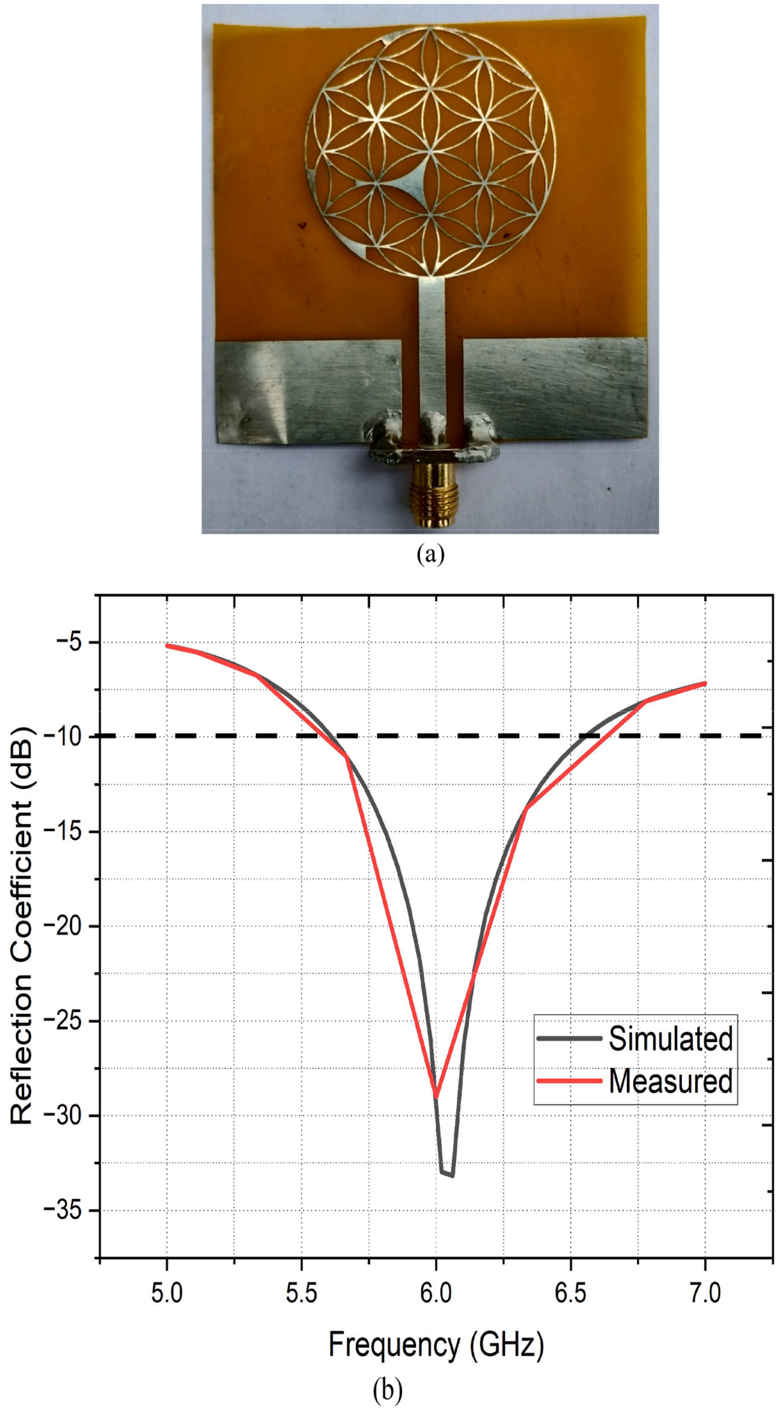

Fig. 5. (a) Fabricated prototype of the proposed flexible CP antenna, (b) simulated and measured reflection coefficient.

highlights the antenna's ability to withstand mechanical deformation without significant changes in its tuning characteristics.

Fig. 9(b) displays the antenna's gain as a function of frequency for the same bending conditions. Although the gain values exhibit slight variations with bending, they consistently remain within the range of 4.0 to 4.9 dBi, indicating stable performance. These gain trends imply that despite minor fluctuations, the antenna sustains sufficient radiation efficiency across the frequency range, even under mechanical stress. The stability observed in both the reflection coefficient and gain confirms the antenna's reliable performance and makes it well-suited for applications that require flexibility and conformal integration.

Fig. 9(c) shows the bending analysis of a flexible antenna, illustrating its axial ratio across different bending angles (0°, 30°, 45°, and 60°) from 5.0 to 6.5 GHz. The axial ratio remains consistently low, between 1.6 and 2.1 dB, indicating strong circular polarization even under mechanical stress. Despite minor fluctuations with bending, the antenna maintains stable polarization performance, proving its suitability for flexible applications where consistent circular polarization is essential.

2.3. Placement analysis

Fig. 10(a) and (b) illustrate the 3D far-field radiation patterns of an antenna mounted on a vehicle, with two different placement positions: on the top roof and the side mirror. In both cases, the radiation pattern is

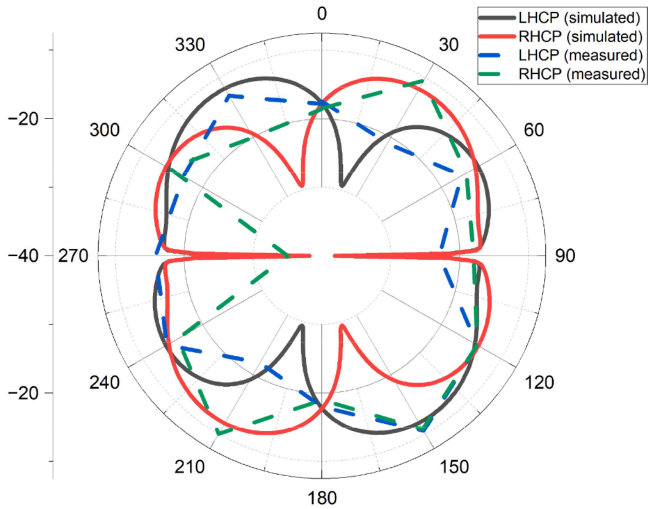

Fig. 6. Simulated and measured far-field pattern of the proposed flexible antenna.

distorted due to the vehicle structure, but the top roof placement shows a more symmetric pattern, likely due to fewer obstructions and a more uniform surrounding environment. The mirror-mounted antenna exhibits a more asymmetric pattern, likely due to the proximity of the vehicle's body, which introduces significant reflection and scattering, leading to a distortion in gain and radiation direction. This comparison helps assess how the antenna's performance is affected by its location on the vehicle, which can be critical for communication and sensing applications.

The proposed antenna demonstrates several advantages over the antennas in the literature as listed in Table 2. It features a significantly lower profile with an ultra-thin thickness of just 0.1 mm, making it the most compact and lightweight design compared to others. Unlike the antennas in [22–28], which are rigid, the proposed antenna is flexible, making it suitable for conformal and wearable applications. Additionally, it achieves a competitive axial ratio bandwidth of 5.5–6.5 GHz, covering its entire operating spectrum. In contrast, some existing designs have a narrower axial ratio bandwidth or lack circular polarization altogether, such as [28]. Although some antennas like [26] offer higher peak gain, they come at the cost of considerably larger dimensions and inflexibility. The proposed antenna achieves a well-balanced trade-off between size, bandwidth, gain, and flexibility, making it a superior choice for modern compact and flexible communication systems.

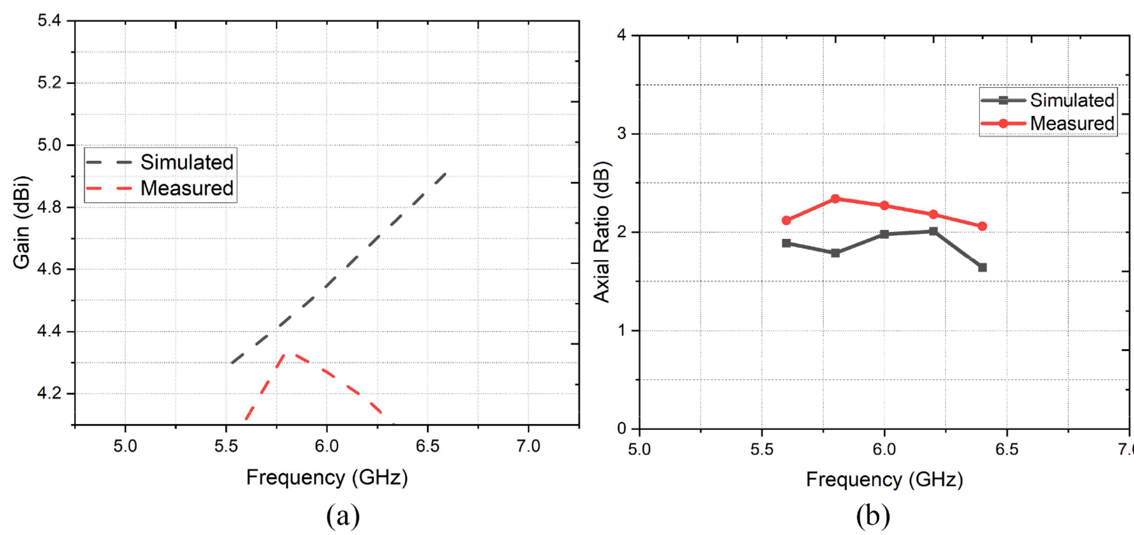

Fig. 7. Simulated and measured (a) Gain, (b) Axial Ratio.

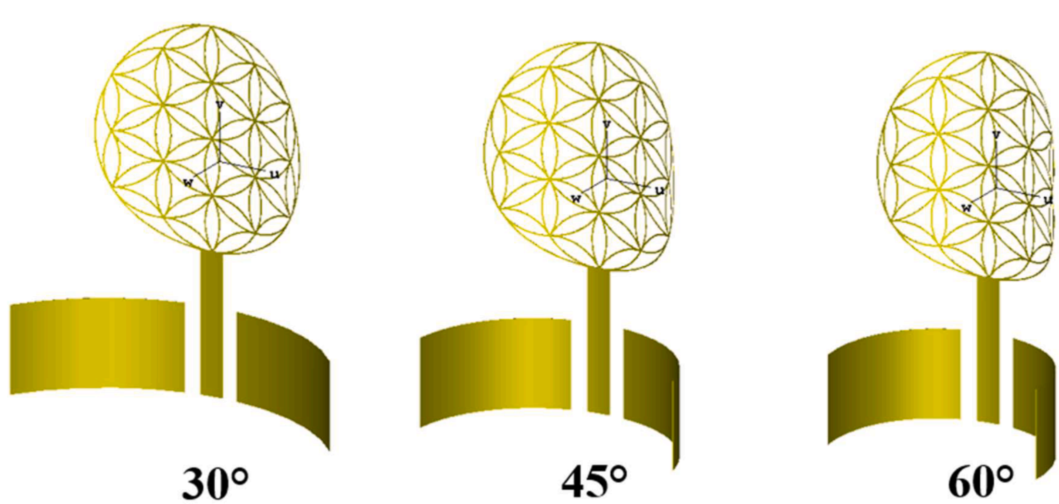

Fig. 8. Flexibility positions of the proposed antenna when angles at (a) 30°, (b) 45°, (c) 60°.

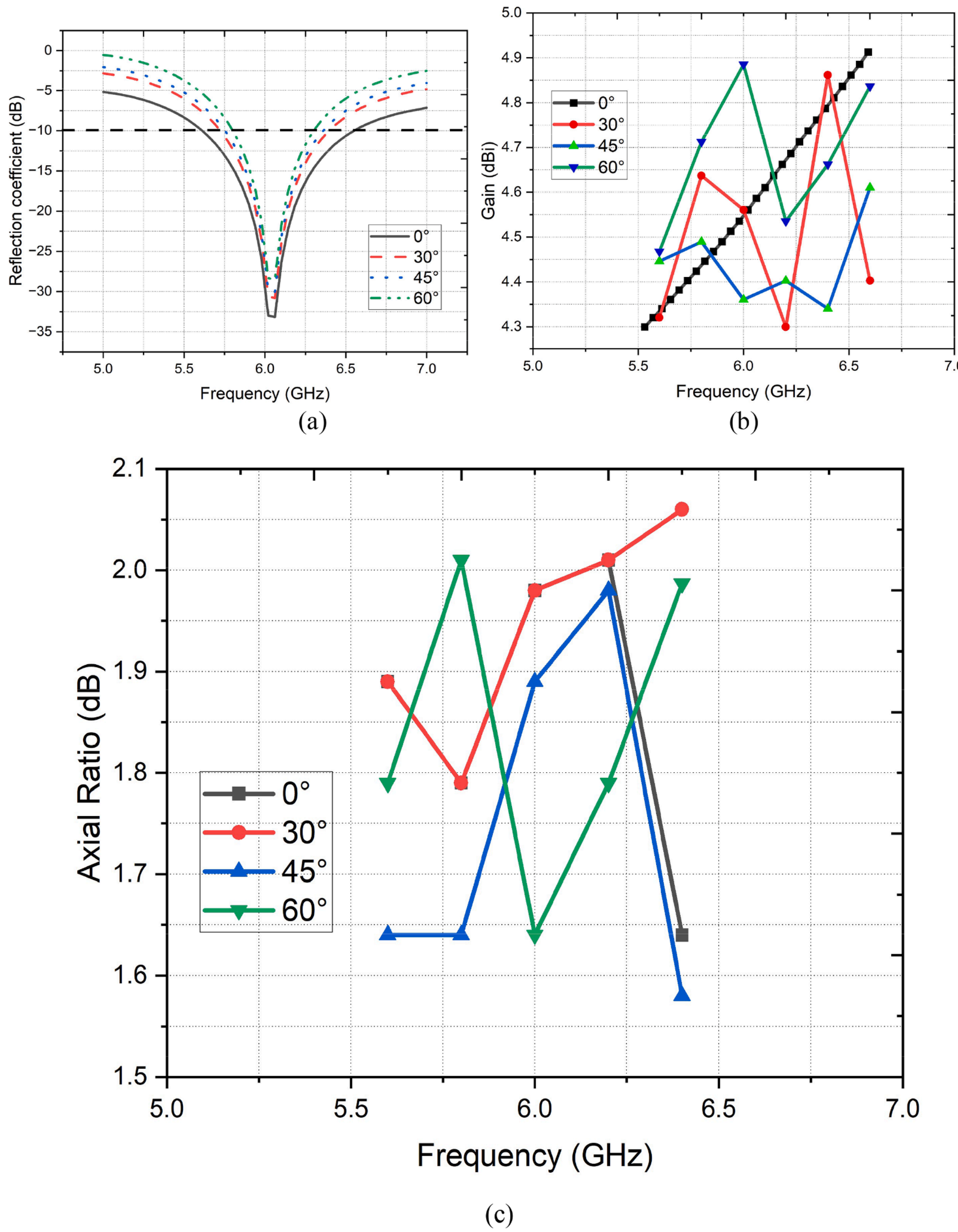

Fig. 9. Conformal analysis of the proposed antenna, (a) Reflection coefficient, (b) Gain, (c) Axial ratio.

3. Conclusion

This research successfully designed, fabricated, and evaluated a highly flexible CPW-fed antenna intended for vehicular communication systems. The antenna, with its compact dimensions of 27.5 × 53 × 0.1 mm^3, demonstrated an impressive measured impedance bandwidth of 5.5 to 6.5 GHz and achieved a peak gain of 4.45 dBi. These results underscore the antenna's capability to perform efficiently in vehicular applications, where reliable and high-performance communication is crucial. The comprehensive bending analysis, carried out under a range of bending radii, confirmed the antenna's ability to retain stable electrical performance even under significant physical deformation, highlighting its robustness and adaptability for flexible deployment scenarios. The prototype, once fabricated, showed excellent alignment between the measured results and the simulated data, further validating the antenna's design integrity. Moreover, the antenna achieved a 100 % axial ratio bandwidth (ARBW), which ensures highly effective circular polarization an essential feature for consistent signal transmission in dynamic vehicular environments. Overall, the antenna's flexible design, robust performance across a range of conditions, and excellent polarization characteristics make it an ideal candidate for integration into advanced vehicular communication systems, where adaptability and reliability are key requirements for future technological advancements.

Funding

No funding has been received for this research.

CRediT authorship contribution statement

Rajesh Kumar D: Writing – original draft, Software, Methodology, Formal analysis, Conceptualization. **Vaithianathan Venkatesan:**

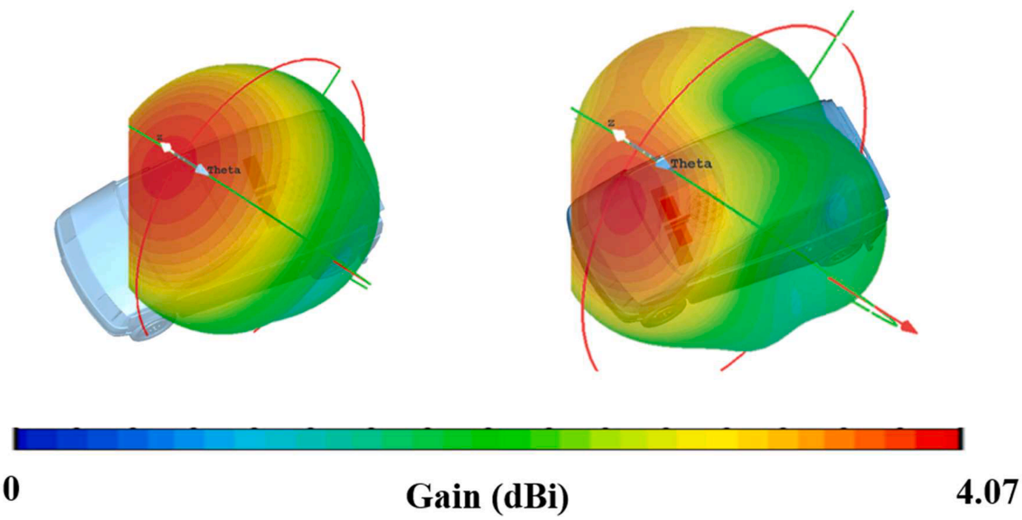

Fig. 10. 3D far-field pattern when the antenna is kept on the vehicle (a) on the top roof, (b) at the mirror.

Table 2
Performance comparison of the proposed antenna with literature.

Ref. No	The overall dimension of the antenna (mm^3)	Operating Spectrum (GHz)	Electrical length of the antenna	Axial Ratio Bandwidth	Peak gain (dBi)	Flexible?
[22]	55 × 49 × 1.5	2–3.5	(0.504 × 0.449 × 0.013)	2.42–3.3 GHz	2.8	No
[23]	100 × 100 × 15	8–8.4	(2.74 × 2.74 × 0.41)	8–8.4	5	No
[24]	Diameter: 238 (6.52) Height: 185 (5.13)	8.025–8.4	Diameter: 238 mm (6.52λ_o) Height: 185 mm (5.13λ_o)	8.025–8.4	5	No
[25]	Diameter: 50 (1.3λ_o) Height: 5.25 (0.137λ_o)	6.8–8.9	Diameter: 50 mm (1.3) Height: 5.25 mm (0.137)	7–8.15	8.6	No
[26]	62 × 62 × 22	8–9.7	(1.77 × 1.77 × 0.63)	8.3–8.88	14	No
[27]	40 × 40 × 1.52	2.57–4.16	(0.44 × 0.44 × 0.17)	3.09–4.13 GHz	3.56	No
[28]	59 × 14 × 0.76	9.4–10.5	(1.96λ_o × 0.46λ_o × 0.025λ_o)	Not Circularly Polarized	9	No
Proposed work	55 × 55 × 0.1	5.5–6.5	0.956 × 1.031 × 0.0034	5.5 – 6.5	4.9	Yes

Writing – original draft, Methodology, Conceptualization. **Raja Periyasamy:** Software, Methodology, Conceptualization. **B. Rubini:** Software, Methodology, Conceptualization. **Ragunath G:** Software, Investigation, Conceptualization. **Om Prakash Kumar:** Writing – review & editing, Supervision, Conceptualization. **Shweta Vincent:** Writing – review & editing, Supervision, Conceptualization.

Declaration of competing interest

The authors declare that they have no known competing financial interests or personal relationships that could have appeared to influence the work reported in this paper.

Acknowledgement

This research contributes to the advancement of vehicular communication technologies, directly supporting Sustainable Development Goal 9 (SDG 9) and SDG 11.

Data availability

The data used to support the findings of this study are included in the article. Data will be made available on request from Rajesh Kumar D.

References

[1] Q.H. Abbasi, R. Gharaei, S.U. Rehman, Recent advances in fabrication methods for flexible antennas in wearable devices: state of the art, Sensors 19 (10) (2023) 2312.
[2] Q. Wang, J. Yang, Design and optimization of a flexible CPW-fed antenna for 5G wearable applications, IEEE Trans. Antennas. Propag. 71 (3) (2023) 1342–1351.
[3] H. Zhang, X. Li, Flexible antenna systems for IoT applications: design, challenges, and future perspectives, IEEE Access. 10 (2022) 39452–39464.
[4] W. Chen, X. Zhao, Polymer-based flexible antennas for wearable devices: a review of recent advances, Prog. Electromagn. Res.. 178 (2023) 91–103.
[5] Y. ie, T Wang, Highly stretchable graphene-based antennas for flexible electronics, Adv. Mater. 35 (12) (2023) 2211–2219.
[6] H. Luo, S. Yeo, Dual-band flexible antenna using liquid metal for 5G communications, IEEE Trans. Microw. Theory. Tech. 71 (6) (2023) 2132–2141.
[7] C. Li, X. Zhang, Flexible antennas for wearable biomedical applications: a review, Biomed. Eng. Lett. 12 (4) (2022) 283–295.
[8] Z. Zhou, Y. Li, Flexible multi-band antennas for IoT devices, IEEE J. Emerg. Sel. Top. Circuits. Syst. 13 (2) (2023) 98–106.
[9] Z. Yuan, F. Wu, Highly efficient flexible antenna for wearable smart devices, J. Electromagn. Waves. Appl. 37 (6) (2023) 872–882.
[10] Q. Wang, J. Yang, Design and optimization of a flexible CPW-fed antenna for 5G wearable applications, IEEE Trans. Antennas. Propag. 71 (3) (2023) 1342–1351.
[11] Y. Xie, T. Wang, Highly stretchable graphene-based antennas for flexible electronics, Adv. Mater. 35 (12) (2023) 2211–2219.
[12] Y. Guo, J. Zhang, Printed flexible antennas for millimeter-wave communications, Microw. Opt. Technol. Lett. 65 (3) (2023) 668–675.
[13] Z. Yuan, F. Wu, Highly efficient flexible antenna for wearable smart devices, J. Electromagn. Waves. Appl. 37 (6) (2023) 872–882.
[14] W. Chen, X. Zhao, Polymer-based flexible antennas for wearable devices: a review of recent advances, Prog. Electromagn. Res.. 178 (2023) 91–103.
[15] Q.H. Abbasi, R. Gharaei, S.U. Rehman, Recent advances in fabrication methods for flexible antennas in wearable devices: state of the art, Sensors 19 (10) (2023) 2312, https://doi.org/10.3390/s19102312.
[16] C. Li, X. Zhang, Flexible antennas for wearable biomedical applications: a review, Biomed. Eng. Lett. 12 (4) (2022) 283–295.
[17] Walid En-Naghma, Hanan Halaq, Abdelghani El Ougli, Analysis, design, and optimization based on genetic algorithms of a highly efficient dual-band rectenna system for radiofrequency energy-harvesting applications, Results. Eng. 23 (2024) 102739.

[18] En-Naghma Walid, Halaq Hanan, An improvement performance of a novel triple-band microstrip antenna design based on a hexagonal patch and truncation in the ground for RF energy harvesting systems, in: 2024 International Conference on Circuit, Systems and Communication (ICCSC), IEEE, 2024.

[19] En-Naghma, Walid, Hanan Halaq, and Abdelghani El Ougli. "Design, and optimization using genetic algorithms of a dual-band microstrip antenna." *Digital Technologies and Applications: Proceedings of ICDTA'24,* Benguerir, Morocco*, Volume* 4 4 (2024): 96.

[20] Deepthi Mariam John, et al., A wideband highly flexible CPW-fed antenna based on characteristic mode analysis for 5G wireless wearable sensor applications, Results. Eng. 23 (2024) 102412.

[21] Salah-Eddine Didi, et al., Creation of a soft circular patch antenna for bio-medical applications for 5G at frequency 2.45 GHz, Results. Eng. 22 (2024) 102319.

[22] T. Huang, G.-B. Liu, H.-F. Zhang, L. Zeng, A new adjustable frequency waveguide circularly polarized antenna based on the solid-state plasma, Applied Physics A 125 (2019) 1–9.

[23] J. Fouany, M. Thevenot, E. Arnaud, F. Torres, C. Menudier, T. Monediere, K. Elis, New concept of telemetry X-band circularly polarized antenna payload for CubeSat, IEEE Antennas. Wirel. Propag. Lett. 16 (2017) 2987–2991.

[24] E. Arnaud, J. Dugenet, K. Elis, A. Girardot, D. Guihard, C. Menudier, T. Monediere, F. Roziere, M. Thevenot, Compact isoflux X-band payload telemetry antenna with simultaneous dual circular polarization for LEO satellite applications, IEEE Antennas. Wirel. Propag. Lett. 19 (10) (2020) 1679–1683.

[25] S. Genovesi, F.A. Dicandia, Characteristic modes analysis of a near-field polarization-conversion metasurface for the design of a wideband circularly polarized X-band antenna, IEEE Access. 10 (2022) 88932–88940.

[26] L. Leszkowska, M. Rzymowski, K. Nyka, L. Kulas, High-gain compact circularly polarized X-band superstrate antenna for CubeSat applications, IEEE Antennas. Wirel. Propag. Lett. 20 (11) (2021) 2090–2094.

[27] A. Altaf, Y. Yang, K.-Y. Lee, K.C. Hwang, Wideband circularly polarized spidron fractal slot antenna with an embedded patch, Int. J. Antennas. Propag. 2017 (2017).

[28] D. El Khamlichi, N.A. Touhami, T. Elhamadi, M.A. En Nasar, High-gain and broadband SIW Cavity-backed slots antenna for X-band applications, Int. J. Microw. Wirel. Technol. 13 (10) (2021) 1078–1085.